

Mixed phosphine/carbonyl derivatives of heterobimetallic copper–iron and copper–tungsten catalysts



Noel J. Leon¹, Hsien-Cheng Yu¹, Thomas J. Mazzacano, Neal P. Mankad^{*}

Department of Chemistry, University of Illinois at Chicago, 845 W. Taylor St., Chicago, IL 60607, USA

ARTICLE INFO

Article history:

Received 3 August 2018

Accepted 24 September 2018

Available online 29 September 2018

Keywords:

Heterobimetallic

Borylation

Copper

Iron

Tungsten

ABSTRACT

Evolution of dihydrogen was observed from reactions of protic metal–hydride complexes $\text{FeCp}(\text{CO})(\text{PR}_3)\text{H}$ and $\text{WCp}^*(\text{CO})_2(\text{PR}_3)\text{H}$ with hydridic $(\text{NHC})\text{CuH}$ complexes, providing access to several heterobimetallic $(\text{NHC})\text{Cu}-\text{FeCp}(\text{CO})(\text{PR}_3)$ and $(\text{NHC})\text{Cu}-\text{WCp}^*(\text{CO})_2(\text{PR}_3)$ complexes that are the mixed phosphine/carbonyl derivatives of previously studied catalysts for C–H borylation (NHC = *N*-heterocyclic carbene). The new complexes were characterized by multinuclear NMR spectroscopy, FT-IR spectroscopy, and in some cases X-ray crystallography. In one case, a $(\text{NHC})\text{Cu}(\mu_2\text{-H})_2\text{FeCp}(\text{PPh}_3)$ complex was structurally characterized as the decomposition product of an unstable $(\text{NHC})\text{Cu}-\text{FeCp}(\text{CO})(\text{PPh}_3)$ derivative. Preliminary trials in C–H borylation catalysis are reported, including measurable activity under photochemical conditions.

© 2018 Elsevier Ltd. All rights reserved.

1. Introduction

Construction of complex organic scaffolds from simpler building blocks generally relies on the presence of reactive heteroatom functional groups or unsaturated bonds. Using ubiquitous C–H positions directly in coupling reactions is comparatively desirable because it greatly reduces the number of synthetic steps by circumventing the need for pre-installed functionalities [1–6]. However, the thermodynamic stability and kinetic inertness of C–H bonds present great challenges to be overcome, as does the problem of site selectivity in organic substrates containing multiple distinct C–H sites. In this regard, transition metal-catalyzed C–H borylation is one of the most promising technologies to emerge recently [7,8]. In this transformation, C–H bonds are converted directly to organoboron esters that, in turn, can be used in the Suzuki–Miyaura reaction or translated into a plethora of other functional groups [9]. Crucially, the C–H borylation reaction obeys well-defined site-selectivity rules guided primarily by C–H acidity or steric accessibility, and catalysts have been developed that facilitate mild reaction conditions. These qualities are best displayed with C–H borylation catalysts based on the precious metal, Ir, ligated by diphosphine, bipyridine, and pincer systems. Recent advances have been made with catalytic C–H borylation using non-precious metals such as Fe [10–12], Ni [13], and Co [14–18],

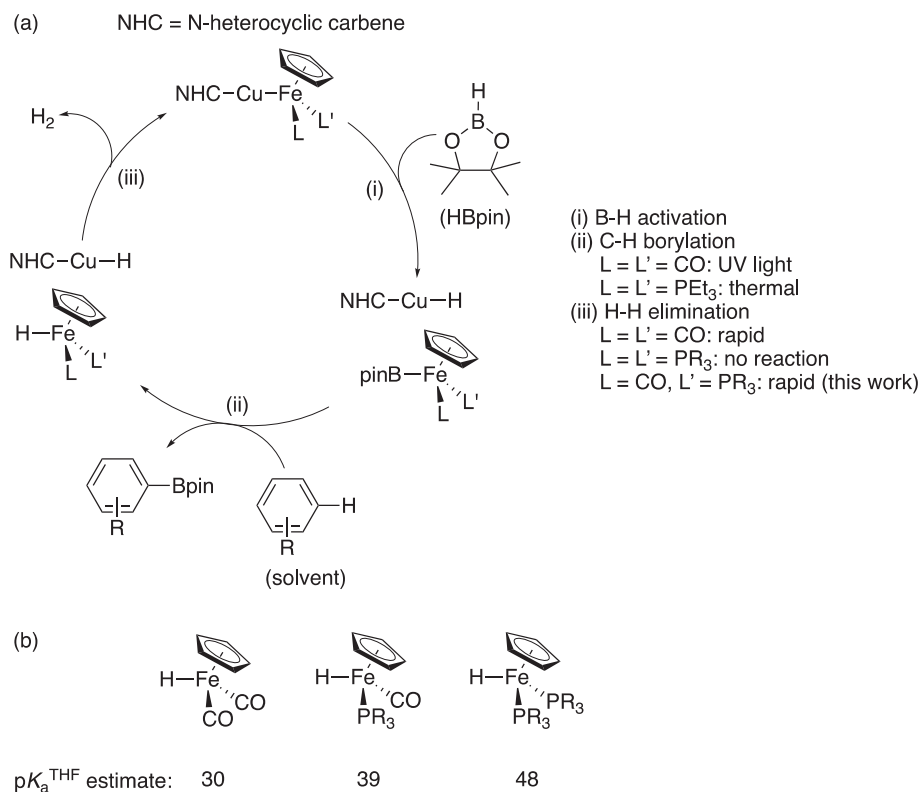
as well as with a metal-free strategy employing frustrated Lewis pairs [19]. While promising, these non-precious metal systems typically exhibit efficient reactivity only for highly activated and/or acidic C–H bonds and require solvent quantities of substrate in order for borylation of unactivated C–H bonds to occur. Thus, more work is required to access non-precious metal catalysts for efficient borylation of unactivated C–H bonds in stoichiometric quantities.

A long term goal of our research group is to use the cooperative behavior of heterobimetallic catalysts to uncover catalytic transformations with non-precious metals that complement single-site precious metal systems [21–23]. One of our first forays into this area involved the discovery that $(\text{IPr})\text{Cu}-\text{FeCp}(\text{CO})_2$ [24], and later $(\text{IPr})\text{Cu}-\text{WCp}^*(\text{CO})_3$ [25], are active catalysts for borylation of arene solvents upon exposure to UV light with a 450-W Hg lamp over 24 h (IPr = *N,N'*-bis(2,6-diisopropylphenyl)imidazol-2-ylidene). These systems rely on the known stoichiometric borylation activity of $\text{FeCp}(\text{CO})_2\text{B}(\text{OR})_2$ and $\text{WCp}^*(\text{CO})_3\text{B}(\text{OR})_2$ intermediates under UV irradiation conditions that was studied in detail by Hartwig many years ago (Scheme 1a, step ii) [26–28]. In our heterobimetallic system, the copper–carbene unit acts as a hydride shuttle that allows for the active Fe- or W-based borylating agents to be continuously regenerated catalytically via cooperative heterobimetallic B–H activation and H–H elimination reactions that occur thermally (Scheme 1a, steps i and iii) [29]. Because the C–H borylation step (Scheme 1a, step ii) is known to involve photochemical CO dissociation [30], we have been targeting a thermal C–H borylation catalyst by replacing one or more CO ligands with labile phosphines

* Corresponding author.

E-mail address: npm@uic.edu (N.P. Mankad).

¹ These authors contributed equally.



Scheme 1. (a) Summary of heterobimetallic C–H borylation catalysis; (b) estimates of [Fe]–H pK_a values in THF based on ligand acidity constants [20]. A similar scheme is operative for (NHC)Cu–WCp(CO)₂L analogues (L = CO or PR₃).

[31]. We were able to demonstrate that FeCp(PEt₃)₂Bpin mediates stoichiometric, UV-free borylation of arene solvents at 70–80 °C due to thermal PEt₃ lability from this sterically crowded complex, but catalysis was precluded because heterobimetallic H–H elimination from (IPr)CuH + FeCp(PEt₃)₂H (Scheme 1a, step iii) did not occur readily [32]. Our hypothesis is that this H–H elimination step requires a highly polarized system where a hydridic [Cu]–H species reacts with a protic [Fe]–H species [33]. Indeed, while FeCp(CO)₂H is known to be significantly protic in character, the FeCp(PEt₃)₂H analogue is less acidic by ~18 pK_a units (Scheme 1b) [20]. This has led us to target mixed phosphine/carbonyl catalysts of the type (NHC)Cu–FeCp(CO)(PR₃), which we hope will mediate thermal C–H borylation while facilitating catalytic turnover via FeCp(CO)(PR₃)H intermediates with more protic character (Scheme 1b). Synthesis and characterization of such mixed phosphine/carbonyl catalysts are reported in this manuscript, as is the demonstration that heterobimetallic H–H elimination does indeed proceed as expected when at least one carbonyl ligand is present in the system.

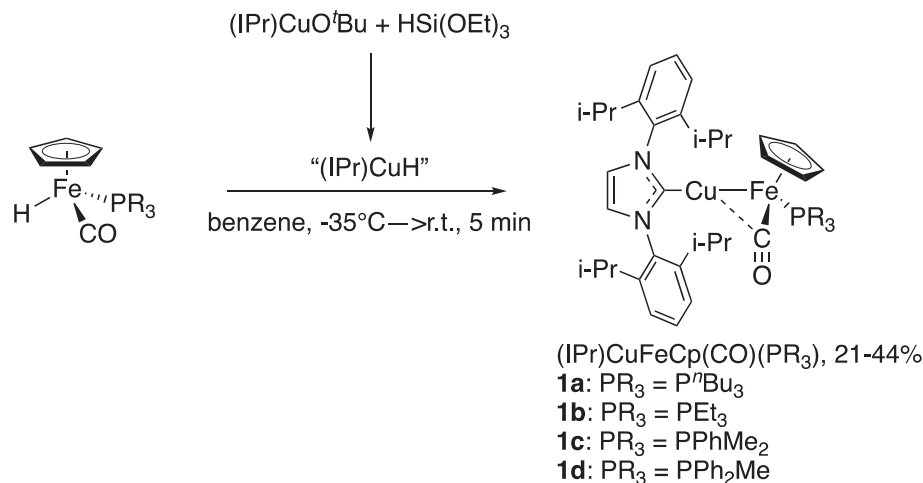
2. Results and discussion

The iron hydride complexes FeCp(CO)(PR₃)H were observed to react rapidly within 5 min with *in situ*-generated (IPr)CuH to release H₂ and provide (IPr)Cu–FeCp(CO)(PR₃) complexes (**1a–d**, Scheme 2). In typical reactions, the crude product mixtures contained a minor side-product tentatively identified as CpFe(IPr)(CO)H (hydride signal: –17.35 ppm) by comparison to the Ru analogue [33], and complexes **1a–d** could be isolated in 21–44% recrystallized yield. Not only does this dehydrogenation reaction provide a synthetic method for these new mixed phosphine/carbonyl heterobimetallic complexes, but it provides further indication that the catalytically relevant H₂ elimination step (Scheme 1, step iii) is

viable if the [Fe]–H pK_a is low enough. Complexes **1a–d** were characterized by multinuclear NMR spectroscopy and FT-IR spectroscopy. X-ray crystallography data was obtained for complexes **1b** and **1d**. Vibrational data for the carbonyl ligands and selected bond metrics are shown in Table 1 for comparison to (IPr)Cu–FeCp(CO)₂ [34,35], and solid-state structures are depicted in Fig. 1. Unlike the thermally stable (IPr)Cu–FeCp(CO)₂ derivative, the mixed phosphine/carbonyl derivatives **1a–d** decompose at a measurable rate (2–12 h at room temperature, see Supplementary Material), which we expect will limit their utility as catalysts.

The accumulated data indicate, as expected, that phosphine ligation renders the Fe centers more electron-rich than in the parent (IPr)Cu–FeCp(CO)₂ derivative. This is particularly evident by examination of the carbonyl stretching frequencies for complexes **1a–d**, which are in the 1791–1813 cm^{–1} range and shifted to significantly lower energy than those of (IPr)Cu–FeCp(CO)₂ (Table 1). Both **1b** and **1d** feature semibridging carbonyl ligands [37], which is indicated by van der Waals Cu···C_{CO} contact and confirmed by tabulation of Curtis's α parameter being 0.39 in both cases and thus in between the bridging CO ($\alpha \leq 0.1$) and terminal CO ($\alpha \geq 0.6$) regimes [38]. The impact on metal–metal bonding of the increased electron density at Fe is a slight contraction of the Cu–Fe distance. Based on our model from previous spectroscopic and computational studies [39], we propose that the modestly shortened Cu–Fe distances in **1b** and **1d** result from enhanced donation in the Fe → Cu dative bond. No significant deviations in C_{NHC}–Cu–Fe angle were observed, indicating that a single phosphine ligand does not provide sufficient steric pressure to strain the metal–metal bond.

When our synthetic method was used to target (IPr)Cu–FeCp(CO)(PPh₃) (**1e**), we did observe a ³¹P NMR resonance at 89.6 ppm, consistent with initial formation of **1e** by comparison to analogues **1a–d**. However, **1e** appears to be unstable. When we tried to recrystallize **1e**, we only obtained a small amount of



Scheme 2. Synthesis of mixed phosphine/carbonyl Cu–Fe heterobimetallic complexes.

Table 1

Selected data comparisons for Cu–Fe heterobimetallic complexes.

Complex	ν_{CO} (cm ⁻¹)	$d(\text{Cu}–\text{Fe})$ (Å)/FSR ^a	$d(\text{Cu} \cdots \text{CO})$ (Å)	$d(\text{C}–\text{O})$ (Å)	$\angle_{\text{C}_{\text{NHC}}–\text{Cu}–\text{Fe}}$ (°)	$\angle_{\text{Fe}–\text{C}–\text{O}}$ (°)
(IPr)Cu–FeCp(CO) ₂ ^b	1914, 1849	2.3462(5)/1.004	2.423(3), 2.749(3)	1.169(3)	170.16(7)	177.2(2)
(IPr)Cu–FeCp(CO)(P ⁿ Bu ₃) (1a)	1795	n.d. ^c	n.d. ^c	n.d. ^c	n.d. ^c	n.d. ^c
(IPr)Cu–FeCp(CO)(PEt ₃) (1b) ^d	1791	2.3331(9)/0.998	2.378(5)	1.186(6)	169.21(14)	176.5(4)
(IPr)Cu–FeCp(CO)(PPhMe ₂) (1c)	1794	n.d. ^c	n.d. ^c	n.d. ^c	n.d. ^c	n.d. ^c
(IPr)Cu–FeCp(CO)(PPh ₂ Me) (1d) ^e	1813	2.299(2)/0.983	2.440(18)	1.13(2)	170.2(15)	170.2(15)

^a FSR = formal shortness ratio [36].

^b Data from literature Refs. [34,35].

^c n.d. = not determined.

^d Structural data is given for one of two independent molecules in the asymmetric unit of **1b**.

^e R value is 0.34, so the reader should take caution in interpreting metrical parameters.

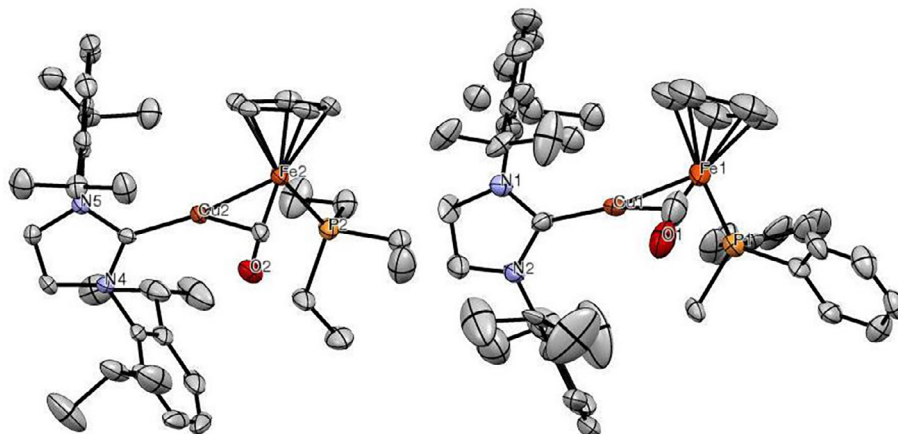


Fig. 1. X-ray crystal structures of **1b** and **1d**, with ellipsoids shown at the 50% probability level. Hydrogen atoms and co-crystallized solvent molecules have been omitted, and only one of two independent molecules in the asymmetric unit of **1b** is shown. Selected bond metrics are given in Table 1.

crystals of a decomposition product, whose ³¹P NMR signal was shifted to 94.7 ppm and which was identified as (IPr)Cu(μ-H)₂-FeCp(PPh₃) (**2**, Fig. 2) by X-ray crystallography. We have been unable to synthesize **2** independently or isolate it in large enough quantities for full characterization and reactivity studies. We assume that source of hydrogen during decomposition is the side-product contaminant CpFe(IPr)(CO)H, which was observed in the crude mixture by ¹H NMR. A related complex LCu(μ₂-H)₂WCp₂ (L = β-diketiminato) was reported recently by Crimmin, who formulated its bonding as consisting of a σ-adduct of H₂WCp₂ bound to [LCu] through η²:η²-binding of two W–H

σ-bonds to Cu(I) [40]. By analogy, one view of **2** is as a η²:η²-adduct of anionic [H₂FeCp(PPh₃)]⁻ to cationic [(IPr)Cu]⁺. However, we cannot rule out an alternative representation of heterodinuclear **2** as the η²-adduct of neutral [HFeCp(PPh₃)] bound to neutral [(IPr)CuH]. The H⋯H distance in **2** of 2.0(1) Å is clearly too long to invoke any dihydrogen interaction [41,42].

Related chemistry is available for the tungsten analogues. Slow dihydrogen evolution occurred from the reaction of WCp⁻(CO)₂(PR₃)H complexes with either (IPr)CuH or (6Pr)CuH (6Pr = N, N'-bis(2,6-diisopropylphenyl)-4,5,6,7-tetrahydro-1,3-diazepin-2-ylidene), providing heterobimetallic (NHC)Cu–WCp⁻(CO)₂(PR₃)

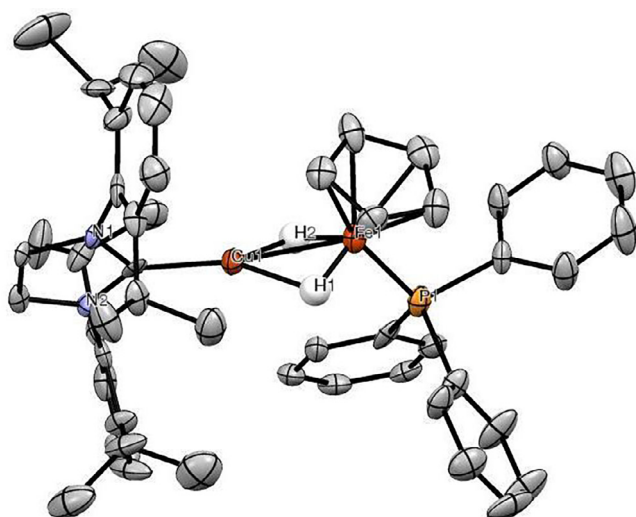


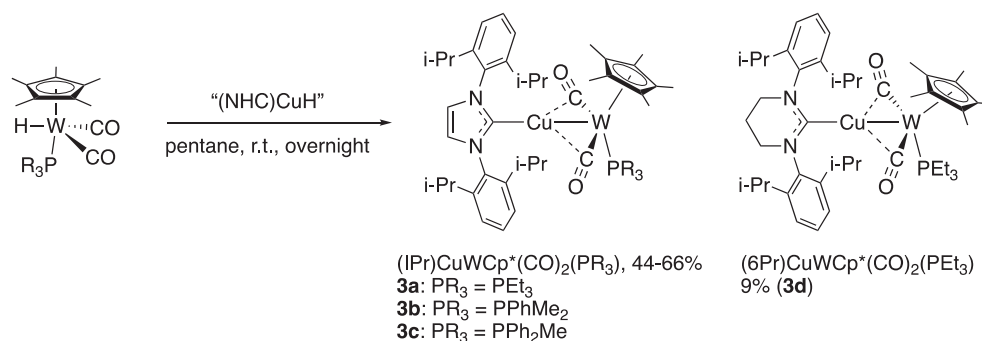
Fig. 2. X-ray crystal structure of **2**, with ellipsoids shown at the 50% probability level. C–H hydrogens are omitted. H1 and H2 were located in the Fourier difference map and refined isotropically. Selected distances (Å): Cu1–Fe1, 2.3652(16); Cu1–H1, 1.76(5); Cu1–H2, 1.68(4); Fe1–H1, 1.39(6); Fe1–H2, 1.70(6); H1–H2, 2.0(1).

complexes in 15–66% yield (**3a–d**, Scheme 3). The observed reactivity is consistent with the estimated pK_a^{THF} values of 14 for $\text{WCp}^+(\text{CO})_2(\text{PR}_3)\text{H}$ [43]. These complexes were characterized by multinuclear NMR spectroscopy and FT-IR spectroscopy, and derivatives **3b–d** were characterized by X-ray crystallography. Relevant data is shown in Table 2 for comparison to $(\text{IPr})\text{Cu–WCp}(\text{CO})_3$, and solid-state structures for **3b–c** are depicted in Fig. 3.

Unlike iron analogues **1a–d**, the tungsten complexes **3a–d** are quite robust thermally and do not decompose upon prolonged heating at 67 °C.

The overall trends for the Cu–W series are similar to those noted above for the Cu–Fe series. The W center is, as expected, more electron-rich upon phosphine ligation in **3a–d**, whose carbonyl stretching frequencies are shifted to lower energies from the corresponding features in $(\text{IPr})\text{Cu–WCp}(\text{CO})_3$ (Table 2). Both **3b** and **3d** feature a pair of semibridging carbonyl ligands according to their α parameters of ~ 0.13 – 0.15 . Complex **3c** has one semibridging carbonyl ligand ($\alpha = 0.14$) and one carbonyl ligand that borders on fully bridging ($\alpha = 0.10$). The metal–metal bonding appears not to be impacted significantly by phosphine ligation, as the Cu–W distances in **3b–d** are all very similar to that of $(\text{IPr})\text{Cu–WCp}(\text{CO})_3$, with no clear trend emerging. This observation is consistent with greater delocalization of extra electron density at W into two carbonyls rather than one for Fe, thus providing very little available electron density for increased donation in the $\text{W} \rightarrow \text{Cu}$ dative bond. Once again, no evidence for steric pressure is observed structurally, as the $\text{C}_{\text{NHC}}\text{–Cu–W}$ angles remain linear regardless of the ligands bound to W.

Due to their higher thermal stability the copper-tungsten complexes were pursued for C–H borylation catalysis in favor of the copper-iron analogues. Under UV irradiation conditions, complexes **3b–d** exhibited some activity for catalyzing borylation of benzene- d_6 solvent with pinacolborane (HBpin). However, the photochemical activity for **3b–d** was very poor (e.g., 27% conversion to $\text{C}_6\text{D}_5\text{Bpin}$ with 20 mol% **3c** under UV irradiation with 450-W Hg lamp over 24 h at room temperature) compared to that observed for the parent $(\text{IPr})\text{CuWCp}^+(\text{CO})_3$ (80% conversion to $\text{C}_6\text{D}_5\text{Bpin}$ under identical conditions with 10 mol% catalyst) [25]. Even the modest photochemical C–H borylation activity with the mixed phosphine/carbonyl catalysts indicates that they are



Scheme 3. Synthesis of mixed phosphine/carbonyl Cu–W heterobimetallic complexes.

Table 2
Selected data comparisons for Cu–W heterobimetallic complexes.

Complex	ν_{CO} (cm ⁻¹)	$d(\text{Cu–W})$ (Å)/FSR ^a	$d(\text{Cu} \cdots \text{CO})$ (Å)	$d(\text{C–O})$ (Å)	$\angle_{\text{C}_{\text{NHC}}\text{–Cu–W}}$ (°)	$\angle_{\text{W–C–O}}$ (°)
$(\text{IPr})\text{Cu–WCp}(\text{CO})_3$ ^{b,c}	1920, 1818, 1784	2.5599(6)/1.035	2.294(7), 2.280(5), 3.858(6)	1.174(8), 1.16(1), 1.159(7)	165.7(1)	173.5(5)
$(\text{IPr})\text{Cu–WCp}^+(\text{CO})_2(\text{PEt}_3)$ (3a)	1750, 1691	n.d. ^d	n.d. ^d	n.d. ^d	n.d. ^d	n.d. ^d
$(\text{IPr})\text{Cu–WCp}^+(\text{CO})_2(\text{PPhMe}_2)$ (3b)	1778, 1702	2.5490(8)/1.031	2.205(2), 2.227(2)	1.197(2), 1.204(2)	178.02(5)	171.6(1), 172.1(1)
$(\text{IPr})\text{Cu–WCp}^+(\text{CO})_2(\text{PPh}_2\text{Me})$ (3c) ^c	1762, 1693	2.579(1)/1.043	2.15(1), 2.18(1)	1.17(2), 1.19(2)	178.8(3)	167.6(9), 168(1)
$(6\text{Pr})\text{Cu–WCp}^+(\text{CO})_2(\text{PEt}_3)$ (3d)	1753, 1688	2.6137(5)/1.057	2.2022(7), 2.2143(7)	1.1801(7), 1.1849(8)	177.37(3)	168.58(5), 170.60(5)

^a FSR = formal shortness ratio [36].

^b Data from literature Ref. [35].

^c Structural data is given for one of two independent molecules in the asymmetric units of $(\text{IPr})\text{CuWCp}(\text{CO})_3$ and **3c**.

^d n.d. = not determined.

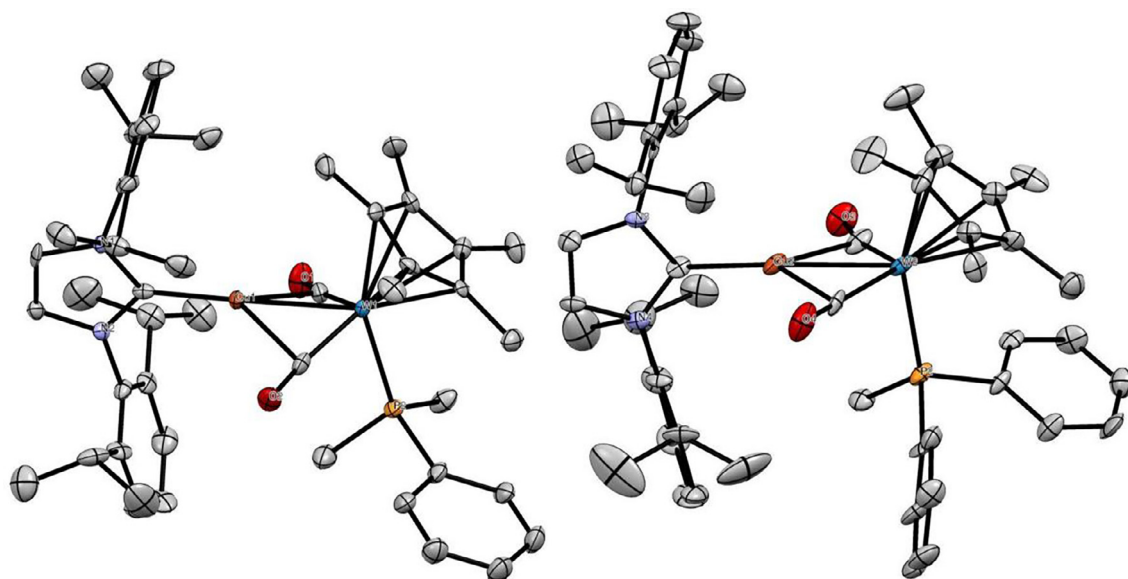


Fig. 3. X-ray crystal structures of **3b** and **3c**, with ellipsoids shown at the 50% probability level. Hydrogen atoms have been omitted, and only one of two independent molecules in the asymmetric unit of **3c** is shown. Selected bond metrics are given in Table 2.

capable of performing the thermal B–H cleavage and H–H elimination reactions required for catalysis (Scheme 1, steps i and iii), and also that they furnish $WCp^*(CO)_2(PR_3)Bpin$ intermediates that are active for arene borylation when provided enough energy to induce ligand dissociation. Unfortunately, under UV-free conditions, no evidence for any catalytic activity was observed for borylation of arene solvents at temperatures up to 110 °C. While disappointing, this lack of thermally-induced catalytic activity is consistent with the structural data discussed above. Specifically, the putative $WCp^*(CO)_2(PR_3)Bpin$ intermediates accessed from catalysts **3b–d** are presumably not sterically crowded enough for the phosphine ligand to be labile, and so the C–H functionalization step (Scheme 1, step ii) is inhibited. Attempts at synthesizing bulkier catalysts such as $(IPr)Cu-WCp^*(CO)_2(PPh_3)$ and $(IPr)Cu-WCp^*(CO)_2(PCy_3)$ failed, possibly due to instability imparted by overcrowding.

3. Conclusions

In conclusion, complexes with mixed phosphine/carbonyl ligation provide metal–hydride intermediates with sufficiently low pK_a values that they are capable of engaging in heterobimetallic H_2 evolution with a hydridic (NHC)CuH partner. Using this H_2 evolution reaction as a synthetic method, several $(NHC)Cu-FeCp(CO)(PR_3)$ and $(NHC)Cu-WCp^*(CO)_2(PR_3)$ complexes were synthesized and thoroughly characterized. In one case, a $(NHC)Cu-FeCp(PPh_3)$ complex was found to decay to yield an interesting $(NHC)Cu-(\mu_2-H)_2FeCp(PPh_3)$ decomposition product. While the new copper–tungsten heterobimetallic complexes are active for photochemical C–H borylation, further work is needed to identify complexes with the right steric/electronic balance for thermally-induced catalysis.

4. Materials and methods

General remarks: Unless otherwise noted, all the syntheses were done in a glovebox filled with N_2 or using standard Schlenk line techniques. Glassware was oven-dried prior to use. All the chemicals purchased from commercial vendors were used without further purification. Solvents were dried using a Glass Contour

solvent purification system built by Pure Process Technology, LLC. Deuterated solvents that were packed under Ar were stored over 3-Å molecular sieves and used without further manipulation. Photolysis was conducted using a 450-W Hanovia mercury arc lamp in an immersion well filled with circulating water. $(IPr)CuO^t-Bu$ [44], $[(IPr)CuH]_2$ [44], and $(6Pr)CuH$ [45] were synthesized using previously published literature methods. $CpFeCO(PR_3)I$ [46], $CpFeCO(PR_3)H$ ($R = PEt_3, P^iBu_3, PMe_2Ph, PMePh_2, PPh_3$) [25], and $Cp^*W(CO)_2(PR_3)H$ ($R = PEt_3, PMe_2Ph, PMePh_2$) [47], were all synthesized by adapted literature methods.

Instrumentation: All the NMR spectra were recorded at ambient temperature using either Bruker Avance DPX-400 or Bruker Avance DPX-500 MHz instruments. Mass analyses were performed with an Advion Expression⁺ CMS mass spectrometer using atmospheric pressure chemical ionization (APCI) in selected ion monitoring (SIM) mode. FT-IR spectra were recorded in a glovebox on powder samples using a Bruker ALPHA spectrometer fitted with a diamond-ATR detection unit. Elemental analyses were performed by the Midwest Microlab, LLC, in Indianapolis, IN. Single-crystal X-ray diffraction experiments were performed using a Bruker PHOTON II diffractometer. Data reduction, solution, and refinement was performed by standard methods [48], and CIF files are available as [Supplementary Material](#).

Synthetic Procedure A: Preparation of $(IPr)CuFeCp(CO)(PR_3)$ ($R = PEt_3, P^iBu_3, PMe_2Ph, PMePh_2$) (1a–d**) and $(IPr)Cu(\mu-H)_2FeCp(PPh_3)$ (**2**):** In a nitrogen filled glovebox, $CpFe(CO)(PR_3)H$ (1 equiv.) was dissolved in C_6H_6 (1 mL) and kept the vial in freezer for 10 min. In a separate vial, $(IPr)CuO^tBu$ (1 equiv.) was dissolved in C_6H_6 (10 mL). While stirring, $(EtO)_3SiH$ (1.01 equiv.) was syringed in, turning the solution to a bright yellow color consistent with formation of $[(IPr)CuH]_2$. The $[(IPr)CuH]_2$ solution was pipette-filtered through Celite into the $CpFe(CO)(PR_3)H$ vial. The reaction turned orange brown in 5 min and then the solution was dried *in vacuo*, resulting in an orange-brown precipitate. The solution was extracted with pentane and pipette-filtered through Celite. Crystallization was accomplished by leaving a concentrated solution in pentane at -35 °C.

Preparation of $(IPr)CuFeCp(CO)(PEt_3)$ (1a**):** Following procedure A with $CpFe(CO)(PEt_3)H$ (14.0 mg, 0.0522 mmol) in C_6H_6 (1 mL), $(IPr)CuO^tBu$ (27.4 mg, 0.0522 mmol) in C_6H_6 (1 mL), and $(EtO)_3SiH$

(10.1 μL , 0.0530 mmol) Yield: 17.2 mg, 0.023 mmol, 44%. ^1H NMR (400 MHz, C_6D_6): δ 7.25 (t, $J = 8.0$ Hz, 2H, p -H), 7.12–7.18 (m, 4H, m -H), 6.30 (s, 2H, NCH), 4.01 (s, 5H, Cp), 2.92 (sept., $J = 8.0$ Hz, 2H, $\text{CH}(\text{CH}_3)_2$), 2.80 (sept., $J = 8.0$ Hz, 2H, $\text{CH}(\text{CH}_3)_2$), 1.50 (d, $J = 12.0$ Hz, 6H, $\text{CH}(\text{CH}_3)_2$), 1.49 (d, $J = 12.0$ Hz, 6H, $\text{CH}(\text{CH}_3)_2$), 1.38–1.45 (m, 3H, PCH_2CH_3), 1.09–1.16 (m, 3H, PCH_2CH_3), 1.09 (d, $J = 8.0$ Hz, 6H, $\text{CH}(\text{CH}_3)_2$), 1.08 (d, $J = 8.0$ Hz, 6H, $\text{CH}(\text{CH}_3)_2$), 0.88–0.97 (m, 9H, PCH_2CH_3). $^{31}\text{P}\{^1\text{H}\}$ NMR (162 MHz, C_6D_6): δ 68.49. $^{13}\text{C}\{^1\text{H}\}$ NMR (100 MHz, C_6D_6): δ 221.6 (CO), 179.6 (NCCu), 145.8, 136.0, 130.0, 124.0, 123.8, 121.2, 73.4 (Cp), 28.8, 28.7, 25.2, 25.0, 24.3, 24.2, 23.8, 23.6, 8.7. IR (solid, cm^{-1}): 2961, 2927, 2869, 1791 (ν_{CO}), 1457, 1401, 1326, 1180, 1104, 1003, 943, 799, 758, 730, 680, 533. Satisfactory elemental analysis data was not obtained due to thermal instability of the complex.

Preparation of $(\text{IPr})\text{CuFeCp}(\text{CO})(\text{P}^i\text{Bu}_3)$ (1b**):** Following procedure A with $\text{CpFe}(\text{CO})(\text{P}^i\text{Bu}_3)\text{H}$ (25.0 mg, 0.0709 mmol) in C_6H_6 (1 mL), $(\text{IPr})\text{CuO}^t\text{Bu}$ (37.2 mg, 0.0709 mmol) in C_6H_6 (1 mL), and $(\text{EtO})_3\text{SiH}$ (13.9 μL , 0.0710 mmol). Yield: 23.9 mg, 0.0297 mmol, 42%. ^1H NMR (400 MHz, C_6D_6): δ 7.27 (t, $J = 8.0$ Hz, 2H, p -H), 7.14–7.20 (m, 4H, m -H partial overlap with solvent peak), 6.27 (s, 2H, NCH), 4.00 (s, 5H, Cp), 2.95 (sept., $J = 8.0$ Hz, 2H, $\text{CH}(\text{CH}_3)_2$), 2.79 (sept., $J = 8.0$ Hz, 2H, $\text{CH}(\text{CH}_3)_2$), 1.53 (d, $J = 8.0$ Hz, 6H, $\text{CH}(\text{CH}_3)_2$), 1.51 (d, $J = 16.0$ Hz, 6H, $\text{CH}(\text{CH}_3)_2$), 1.19–1.46 (m, 18H, $\text{P}(\text{CH}_2)_3\text{CH}_3$), 1.10 (d, $J = 8.0$ Hz, 6H, $\text{CH}(\text{CH}_3)_2$), 1.10 (d, $J = 8.0$ Hz, 6H, $\text{CH}(\text{CH}_3)_2$), 0.96 (t, $J = 8.0$ Hz, 9H, $\text{P}(\text{CH}_2)_3\text{CH}_3$). $^{31}\text{P}\{^1\text{H}\}$ NMR (162 MHz, C_6D_6): δ 61.53. $^{13}\text{C}\{^1\text{H}\}$ NMR (100 MHz, C_6D_6): δ 221.7 (CO), 179.6 (NCCu), 145.8, 136.1, 130.1, 124.1, 123.8, 121.2, 73.4 (Cp), 33.2, 33.0, 28.8, 28.7, 26.8, 24.8, 24.7, 24.2, 24.1, 24.0, 23.7, 14.0. IR (solid, cm^{-1}): 2960, 2925, 2866, 1795 (ν_{CO}), 1458, 1406, 1325, 1172, 1109, 946, 936, 801, 757, 733, 708, 573, 535. Satisfactory elemental analysis data was not obtained due to thermal instability of the complex.

Preparation of $(\text{IPr})\text{CuFeCp}(\text{CO})(\text{PMe}_2\text{Ph})$ (1c**):** Following procedure A with $\text{CpFe}(\text{CO})(\text{PMe}_2\text{Ph})\text{H}$ (11.3 mg, 0.0392 mmol) in C_6H_6 (1 mL), $(\text{IPr})\text{CuO}^t\text{Bu}$ (20.5 mg, 0.0392 mmol) in C_6H_6 (1 mL), and $(\text{EtO})_3\text{SiH}$ (7.7 μL , 0.0400 mmol). Yield: 6.7 mg, 0.009 mmol, 23%. ^1H NMR (400 MHz, C_6D_6): δ 7.81–7.85 (m, 2H, PC_6H_5), δ 7.22 (t, $J = 8.0$ Hz, 2H, p -H), 7.13–7.16 (m, 4H, m -H partial overlap with solvent peak), δ 7.11–7.13 (m, 2H, PC_6H_5), δ 7.03–7.06 (m, 1H, PC_6H_5), 6.31 (s, 2H, NCH), 3.93 (s, 5H, Cp), 2.87 (sept., $J = 8.0$ Hz, 2H, $\text{CH}(\text{CH}_3)_2$), 2.80 (sept., $J = 8.0$ Hz, 2H, $\text{CH}(\text{CH}_3)_2$), 1.53 (d, $J = 8.0$ Hz, 6H, $\text{CH}(\text{CH}_3)_2$), 1.49 (d, $J = 8.0$ Hz, 6H, $\text{CH}(\text{CH}_3)_2$), 1.41 (d, $J = 8.0$ Hz, 3H, PCH_3), 1.18 (d, $J = 8.0$ Hz, 3H, PCH_3), 1.10 (d, $J = 8.0$ Hz, 12H, $\text{CH}(\text{CH}_3)_2$). $^{31}\text{P}\{^1\text{H}\}$ NMR (400 MHz, C_6D_6): δ 44.89. IR (solid, cm^{-1}): 2961, 2927, 2868, 1793 (ν_{CO}), 1458, 1401, 1325, 1270, 1179, 1060, 1011, 932, 896, 799, 758, 741, 692, 599, 536. Satisfactory elemental analysis data was not obtained due to thermal instability of the complex.

Preparation of $(\text{IPr})\text{CuFeCp}(\text{CO})(\text{PMePh}_2)$ (1d**):** Following procedure A with $\text{CpFe}(\text{CO})(\text{PMePh}_2)\text{H}$ (66.6 mg, 0.1903 mmol) in C_6H_6 (1 mL), $(\text{IPr})\text{CuO}^t\text{Bu}$ (100.0 mg, 0.1903 mmol) in C_6H_6 (1 mL), and $(\text{EtO})_3\text{SiH}$ (38 μL , 0.1910 mmol). Yield: 32.1 mg, 0.039 mmol, 21%. ^1H NMR (400 MHz, C_6D_6): δ 7.75–7.79 (m, 2H, PC_6H_5), δ 7.54–7.58 (m, 2H, PC_6H_5), δ 7.22 (t, $J = 8.0$ Hz, 2H, p -H), 7.12–7.16 (m, 4H, m -H partial overlap with solvent peak), δ 7.07–7.10 (m, 6H, PC_6H_5), 6.31 (s, 2H, NCH), 3.93 (s, 5H, Cp), 2.93 (sept., $J = 8.0$ Hz, 2H, $\text{CH}(\text{CH}_3)_2$), 2.75 (sept., $J = 8.0$ Hz, 2H, $\text{CH}(\text{CH}_3)_2$), 1.51 (d, $J = 4.0$ Hz, 6H, $\text{CH}(\text{CH}_3)_2$), 1.44 (d, $J = 8.0$ Hz, 3H, PCH_3), 1.35 (d, $J = 8.0$ Hz, 6H, $\text{CH}(\text{CH}_3)_2$), 1.09 (d, $J = 4.0$ Hz, 6H, $\text{CH}(\text{CH}_3)_2$), 1.08 (d, $J = 4.0$ Hz, 6H, $\text{CH}(\text{CH}_3)_2$). $^{31}\text{P}\{^1\text{H}\}$ NMR (162 MHz, C_6D_6): δ 65.56. IR (solid, cm^{-1}): 2959, 2924, 2865, 1813 (ν_{CO}), 1457, 1433, 1325, 1211, 1085, 1064, 1011, 945, 879, 802, 759, 744, 698, 596, 538, 506. Satisfactory elemental analysis data was not obtained due to thermal instability of the complex.

Preparation of $(\text{IPr})\text{Cu}(\mu\text{-H})_2\text{FeCp}(\text{PPh}_3)$ (2**):** Following procedure A with $\text{CpFe}(\text{CO})(\text{PPh}_3)\text{H}$ (24.3 mg, 0.0587 mmol) in C_6H_6 (1 mL),

$(\text{IPr})\text{CuO}^t\text{Bu}$ (31.0 mg, 0.0587 mmol) in C_6H_6 (1 mL), and $(\text{EtO})_3\text{SiH}$ (11.8 μL , 0.0600 mmol). During recrystallization it was found that the decomposition product **2** was produced. Yield: 4.3 mg, 0.005 mmol, 9%. ^1H NMR (400 MHz, C_6D_6): δ 7.70–7.75 (m, 6H, PC_6H_5), δ 7.22 (m, 2H, o -H partial overlap with solvent peak), 7.09 (d, $J = 8.0$ Hz, 4H, m -H), δ 6.93–7.01 (m, 9H, PC_6H_5), 6.19 (s, 2H, NCH), 3.66 (s, 5H, Cp), 2.77 (sept., $J = 8.0$ Hz, 4H, $\text{CH}(\text{CH}_3)_2$), $\text{CH}(\text{CH}_3)_2$, 1.42 (d, $J = 8.0$ Hz, 12H, $\text{CH}(\text{CH}_3)_2$), 1.09 (d, $J = 8.0$ Hz, 12H, $\text{CH}(\text{CH}_3)_2$), -17.77 (d, $J = 40.0$ Hz, 2H, $\mu\text{-H}$). $^{31}\text{P}\{^1\text{H}\}$ NMR (162 MHz, C_6D_6): δ 94.69. IR (solid, cm^{-1}): 2958, 2924, 2867, 1616, 1585, 1471, 1433, 1309, 1268, 1181, 1062, 1000, 988, 942, 803, 745, 694, 530, 516, 496, 474, 449, 422.

Procedure B: Preparation of $(\text{NHC})\text{CuWCP}(\text{CO})_2(\text{PR}_3)$ (3a-c**):** $\text{Cp}^*\text{W}(\text{CO})_2(\text{PR}_3)\text{H}$ was produced by the addition of phosphine (3 equiv.) to a solution of $\text{Cp}^*\text{W}(\text{CO})_3\text{H}$ (1.5 equiv.) in toluene (10 mL) and heating at 110 $^\circ\text{C}$ in a closed vial for three days. The crude product was pumped down *in vacuo* at room temperature until dry and then at 60 $^\circ\text{C}$ for 3 h. The crude material was then dissolved in pentane (10 mL) and stored at -30 $^\circ\text{C}$ overnight. The solution was pipet-filtered through Celite to remove white crystals and used without further purification. In a separate vial, $(\text{NHC})\text{CuO}^t\text{Bu}$ (1 equiv.) was dissolved in pentane (5 mL). While stirring, $(\text{EtO})_3\text{SiH}$ (1 equiv.) was syringed in, turning the solution to a bright yellow color consistent with formation of $[(\text{IPr})\text{CuH}]_2$. The $[(\text{IPr})\text{CuH}]_2$ solution was pipette-filtered through Celite into the solution of $\text{Cp}^*\text{W}(\text{CO})_2(\text{PR}_3)\text{H}$. The reaction was left to stir overnight with slow formation of a dark yellow-orange color. The crude product was recrystallized two times from slow evaporation of pentane solutions in the glovebox freezer at -30 $^\circ\text{C}$ to obtain yellow to red crystals suitable for characterization.

Preparation of $(\text{IPr})\text{CuWCP}(\text{CO})_2(\text{PET}_3)$ (3a**):** Following procedure B, PET_3 (37.6 mg, 0.495 mmol), $\text{Cp}^*\text{W}(\text{CO})_3\text{H}$ (100 mg, 0.247 mmol), $(\text{IPr})\text{CuO}^t\text{Bu}$ (89 mg, 0.17 mmol), and $(\text{EtO})_3\text{SiH}$ (25 μL , 0.17 mmol) were used. Yield: 105 mg, 0.11 mmol, 66%. ^1H NMR (400 MHz, C_6D_6): δ 7.36–7.16 (m, 3H, ArH), 6.41 (s, 2H, NCH), 2.97 (sept., $J = 6.5$ Hz, 4H, $\text{CH}(\text{CH}_3)_2$), 1.96 (s, 15H, Cp^*), 1.58 (d, $J = 6.5$ Hz, 12H, $\text{CH}(\text{CH}_3)_2$), 1.36 (t, $J = 8.0$ Hz, 9H, PCH_2CH_3), 1.08 (d, $J = 6.5$ Hz, 12H, $\text{CH}(\text{CH}_3)_2$), 1.01–0.94 (m, 6H, PCH_2CH_3). $^{31}\text{P}\{^1\text{H}\}$ NMR (162 MHz, C_6D_6): δ 21.24. IR (solid, cm^{-1}): 2957, 2869, 1750 (ν_{CO}), 1691 (ν_{CO}), 1456, 1364, 1330, 1027, 802, 759, 700, 564, 483, 418. Elemental analysis calculated (%) for $[\text{C}_{45}\text{H}_{62}\text{O}_2\text{CuWPN}_2]$: C, 57.41; H, 6.63; N, 2.97; found: C, 57.39; H, 6.88; N, 2.92.

Preparation of $(\text{IPr})\text{CuWCP}(\text{CO})_2(\text{PMe}_2\text{Ph})$ (3b**):** Following procedure B, PMe_2Ph (68.38 mg, 0.495 mmol), $\text{Cp}^*\text{W}(\text{CO})_3\text{H}$ (100 mg, 0.247 mmol), $(\text{IPr})\text{CuO}^t\text{Bu}$ (89 mg, 0.17 mmol), and $(\text{EtO})_3\text{SiH}$ (25 μL , 0.17 mmol) were used. Yield: 96 mg, 0.10 mmol, 60%. ^1H NMR (400 MHz, C_6D_6): δ 7.72 (t, $J = 7.5$ Hz, 2H, ArH), 7.26–7.22 (m, 3H, ArH), 7.16–7.13 (m, 2H, ArH-overlap with solvent) 7.03–6.96 (m, 4H, ArH), 6.45 (s, 2H, NCH), 2.97 (sept., $J = 6.5$ Hz, 4H, $\text{CH}(\text{CH}_3)_2$), 1.80 (s, 15H, Cp^*), 1.61 (d, $J = 6.5$ Hz, 12H, $\text{CH}(\text{CH}_3)_2$), 1.52 (s, 3H, PMe), 1.50 (s, 3H, PMe), 1.10 (d, $J = 6.5$ Hz, 12H, $\text{CH}(\text{CH}_3)_2$), $^{31}\text{P}\{^1\text{H}\}$ NMR (162 MHz, C_6D_6): δ 3.35. IR (solid, cm^{-1}): 3114, 2960, 2906, 2866, 1778 (ν_{CO}), 1702 (ν_{CO}), 902, 800, 743, 698, 677, 573, 483, 427. Repeated attempts at elemental analysis did not give satisfactory results. ^1H and ^{31}P NMR spectroscopy was used to assess purity (see [Supplementary Material](#)).

Preparation of $(\text{IPr})\text{CuWCP}(\text{CO})_2(\text{PMePh}_2)$ (3c**):** Following procedure B, PMePh_2 (99.1 mg, 0.495 mmol), $\text{Cp}^*\text{W}(\text{CO})_3\text{H}$ (100 mg, 0.247 mmol), $(\text{IPr})\text{CuO}^t\text{Bu}$ (89 mg, 0.17 mmol), and $(\text{EtO})_3\text{SiH}$ (25 μL , 0.17 mmol) were used. Yield: 75 mg, 0.073 mmol, 43%. ^1H NMR (400 MHz, C_6D_6): δ 7.72 (t, $J = 7.5$ Hz, 4H, ArH), 7.24–7.12 (m, 10H, ArH), 7.03 (t, $J = 7.0$ Hz, 2H, ArH) 6.42 (s, 2H, NCH), 2.94 (sept., $J = 7.0$ Hz, 4H, $\text{CH}(\text{CH}_3)_2$), 1.78 (s, 15H, Cp^*), 1.75 (d, $J = 8.1$ Hz, 3H, PMe), 1.53 (d, $J = 7.0$ Hz, $\text{CH}(\text{CH}_3)_2$), 1.07 (d, $J = 7.0$ Hz, 12H, $\text{CH}(\text{CH}_3)_2$), $^{31}\text{P}\{^1\text{H}\}$ NMR (162 MHz, C_6D_6): δ 25.64. IR (solid, cm^{-1}): 2962, 2901, 2867, 1762 (ν_{CO}), 1693 (ν_{CO}), 1459,

887, 744, 695, 524, 490, 422. Elemental analysis calculated (%) for $[C_{52}H_{60}O_2CuWPN_2]$ C, 61.03; H, 5.91; N, 2.74; found: C, 60.87; H, 5.91; N, 2.59.

Preparation of 6PrCuWCP⁺(CO)₂(PEt₃) (3d): PEt₃ (32 mg, 0.420 mmol, 2 equiv.) was added to a solution of Cp⁺W(CO)₃H (85 mg, 0.210, 1.5 equiv.) in toluene (10 mL) and heated at 110 °C for three days. The crude product was pumped down *in vacuo* at room temperature until dry and then at 60 °C for 3 h to give 104 mg (0.210 mmol). The crude product was dissolved pentane (10 mL), and 6PrCuH (98 mg, 0.21 mmol) was added. Recrystallization from slow evaporating pentane in the glovebox freezer at –30 °C gave pure product. This product was further recrystallized in slow evaporating pentane to afford crystals for single crystal XRD analysis. Yield: 30 mg, 0.031 mmol, 15%. ¹H NMR (400 MHz, C₆D₆): δ 7.24–7.17 (m, 4H, Ar–H significant overlap with solvent), 3.41 (sept., *J* = 6.7 Hz, 4H, CH(CH₃)₂), 2.92 (t, *J* = 5.7 Hz, 4H, NCH₂CH₂CH₃N) 1.88 (s, 15H, Cp⁺), 1.74 (d, *J* = 6.5 Hz, 12H, CH(CH₃)₂), 1.17 (d, *J* = 6.5 Hz, 12H, CH(CH₃)₂), 1.01–0.94 (m, 9H, PCH₂CH₃), 0.89–0.80 (m, 6H, PCH₂CH₃) ³¹P{¹H} NMR (162 MHz, C₆D₆): δ 20.75. IR (solid, cm⁻¹): 2956, 2930, 2902, 2872, 1753(ν_{CO}), 1688, 1483, 1446, 1321, 1295, 1198, 1026, 803, 758, 700, 641, 604, 560, 410. *m/z* (APCI + SIM mode): 118.1(PEt₃), 135.2(Cp⁺), 404.3(6Pr), 467.2(6PrCu), 493.1(Cp⁺W(CO)₂PEt₃), 960.4(6PrCuCp⁺W(CO)₂PEt₃).

Acknowledgements

Funding was provided by the National Science Foundation (CHE-1664632). Dr. Chia-Wei Hsu assisted with mass spectrometric analysis.

Appendix A. Supplementary data

CCDC 1860130–1860135 contains the supplementary crystallographic data for 1b, 1d, 3b–d. These data can be obtained free of charge via <http://www.ccdc.cam.ac.uk/conts/retrieving.html>, or from the Cambridge Crystallographic Data Centre, 12 Union Road, Cambridge CB2 1EZ, UK; fax: (+44) 1223-336-033; or e-mail: deposit@ccdc.cam.ac.uk. Supplementary data (spectral data) to this article can be found online at <https://doi.org/10.1016/j.poly.2018.09.062>.

References

- J.F. Hartwig, Evolution of C–H bond functionalization from methane to methodology, *J. Am. Chem. Soc.* 138 (2016) 2, <https://doi.org/10.1021/jacs.5b08707>.
- H.M.L. Davies, J. Du Bois, J.-Q. Yu, C–H functionalization in organic synthesis, *Chem. Soc. Rev.* 40 (2011) 1855, <https://doi.org/10.1039/c1cs90010b>.
- K.M. Engle, T.-S. Mei, M. Wasa, J.-Q. Yu, Weak coordination as a powerful means for developing broadly useful C–H functionalization reactions, *Acc. Chem. Res.* 45 (2012) 788, <https://doi.org/10.1021/ar200185g>.
- W.R. Gutekunst, P.S. Baran, C–H functionalization logic in total synthesis, *Chem. Soc. Rev.* 40 (2011) 1976, <https://doi.org/10.1039/c0cs00182a>.
- W.D. Jones, F.J. Feher, Comparative reactivities of hydrocarbon carbon-hydrogen bonds with a transition-metal complex, *Acc. Chem. Res.* 22 (1989) 91, <https://doi.org/10.1021/ar00159a002>.
- W.D. Jones, Enhanced: conquering the carbon-hydrogen bond, *Science* 287 (2000) 1942, <https://doi.org/10.1126/science.287.5460.1942>.
- I.A.I. Mkhallid, J.H. Barnard, T.B. Marder, J.M. Murphy, J.F. Hartwig, C–H activation for the construction of C–B bonds, *Chem. Rev.* 110 (2010) 890, <https://doi.org/10.1021/cr900206p>.
- J.-Y. Cho, M.K. Tse, D. Holmes, R.E. Maleczka, M.R. Smith, Remarkably selective iridium catalysts for the elaboration of aromatic C–H bonds, *Science* 295 (2002) 305, <https://doi.org/10.1126/science.1067074>.
- J.F. Hartwig, Borylation and silylation of C–H bonds: a platform for diverse C–H bond functionalizations, *Acc. Chem. Res.* 45 (2012) 864, <https://doi.org/10.1021/ar200206a>.
- Y. Ohki, T. Hatanaka, K. Tatsumi, C–H bond activation of heteroarenes mediated by a half-sandwich iron complex of N-heterocyclic carbene, *J. Am. Chem. Soc.* 130 (2008) 17174, <https://doi.org/10.1021/ja8063028>.
- T. Hatanaka, Y. Ohki, K. Tatsumi, CH bond activation/borylation of furans and thiophenes catalyzed by a half-sandwich iron N-heterocyclic carbene complex, *Chem. Asian J.* 5 (2010) 1657, <https://doi.org/10.1002/asia.201000140>.
- Y. Yoshigoe, Y. Kuninobu, Iron-catalyzed *ortho*-selective C–H borylation of 2-phenylpyridines and their analogs, *Org. Lett.* 19 (2017) 3450, <https://doi.org/10.1021/acs.orglett.7b01423>.
- T. Furukawa, M. Tobisu, N. Chatani, Nickel-catalyzed borylation of arenes and indoles via C–H bond cleavage, *Chem. Commun.* 51 (2015) 6508, <https://doi.org/10.1039/c5cc01378j>.
- J.V. Obligation, S.P. Semproni, P.J. Chirik, Cobalt-catalyzed C–H borylation, *J. Am. Chem. Soc.* 136 (2014) 4133, <https://doi.org/10.1021/ja500712z>.
- J.V. Obligation, S.P. Semproni, I. Pappas, P.J. Chirik, Cobalt-catalyzed C(sp²)–H borylation: mechanistic insights inspire catalyst design, *J. Am. Chem. Soc.* 138 (2016) 10645, <https://doi.org/10.1021/jacs.6b06144>.
- J.V. Obligation, P.J. Chirik, Mechanistic studies of cobalt-catalyzed C(sp²)–H borylation of five-membered heteroarenes with pinacolborane, *ACS Catal.* 7 (2017) 4366, <https://doi.org/10.1021/acscatal.7b01151>.
- C.R.K. Jayasundara, D. Sabasovs, R.J. Staples, J. Oppenheimer, M.R. Smith, R.E. Maleczka, Cobalt-catalyzed C–H borylation of alkyl arenes and heteroarenes including the first selective borylations of secondary benzylic C–H bonds, *Organometallics* 37 (2018) 1567, <https://doi.org/10.1021/acs.organomet.8b00144>.
- J.V. Obligation, H. Zhong, P.J. Chirik, Insights into activation of cobalt pre-catalysts for C(sp²)–H functionalization, *Isr. J. Chem.* 57 (2017) 1032, <https://doi.org/10.1002/ijch.201700072>.
- M.-A. Légaré, M.-A. Courtemanche, É. Rochette, F.-G. Fontaine, Metal-free catalytic C–H bond activation and borylation of heteroarenes, *Science* 349 (2015) 513, <https://doi.org/10.1126/science.aab3591>.
- R.H. Morris, Brønsted-Lowry acid strength of metal hydride and dihydrogen complexes, *Chem. Rev.* 116 (2016) 8588, <https://doi.org/10.1021/acs.chemrev.5b00695>.
- N.P. Mankad, Diverse bimetallic mechanisms emerging from transition metal Lewis acid/base pairs: development of co-catalysis with metal carbenes and metal carbonyl anions, *Chem. Commun.* 34 (2018) 5497, <https://doi.org/10.1039/c7cc09675e>.
- M.K. Karunananda, N.P. Mankad, E-selective semi-hydrogenation of alkynes by heterobimetallic catalysis, *J. Am. Chem. Soc.* 137 (2015) 14598, <https://doi.org/10.1021/jacs.5b10357>.
- S. Bagherzadeh, N.P. Mankad, Catalyst control of selectivity in CO₂ reduction using a tunable heterobimetallic effect, *J. Am. Chem. Soc.* 137 (2015) 10898, <https://doi.org/10.1021/jacs.5b05692>.
- T.J. Mazzacano, N.P. Mankad, Base metal catalysts for photochemical C–H borylation that utilize metal-metal cooperativity, *J. Am. Chem. Soc.* 135 (2013) 17258, <https://doi.org/10.1021/ja408861p>.
- T.J. Mazzacano, *Developments in Base Metal-Catalyzed C–H Borylation Ph.D. thesis*, University of Illinois at Chicago, 2017.
- K.M. Waltz, X. He, C. Muhoro, J.F. Hartwig, Hydrocarbon functionalization by transition metal boryls, *J. Am. Chem. Soc.* 117 (1995) 11357.
- K.M. Waltz, C.N. Muhoro, J.F. Hartwig, C–H activation and functionalization of unsaturated hydrocarbons by transition-metal boryl complexes, *Organometallics* 18 (1999) 3383, <https://doi.org/10.1021/om990113v>.
- K.M. Waltz, J.F. Hartwig, Functionalization of alkanes by isolated transition metal boryl complexes, *J. Am. Chem. Soc.* 122 (2000) 11358, <https://doi.org/10.1021/ja002840j>.
- S.R. Parmelee, T.J. Mazzacano, Y. Zhu, N.P. Mankad, J.A. Keith, A heterobimetallic mechanism for C–H borylation elucidated from experimental and computational data, *ACS Catal.* 5 (2015) 3689, <https://doi.org/10.1021/acscatal.5b00275>.
- K.R. Sawyer, J.F. Cahoon, J.E. Shanoski, E.A. Glascoe, M.F. Kling, J.P. Schlegel, M. C. Zorb, M. Hapke, J.F. Hartwig, C.E. Webster, C.B. Harris, Time-resolved IR studies on the mechanism for the functionalization of primary C–H bonds by photoactivated Cp⁺W(CO)₃(Bpin), *J. Am. Chem. Soc.* 132 (2010) 1848, <https://doi.org/10.1021/ja906438a>.
- N. Mankad, Non-precious metal catalysts for C–H borylation enabled by metal-metal cooperativity, *Synlett* 25 (2014) 1197, <https://doi.org/10.1055/s-0033-1340823>.
- T.J. Mazzacano, N.P. Mankad, Thermal C–H borylation using a CO-free iron boryl complex, *Chem. Commun.* 51 (2015) 5379, <https://doi.org/10.1039/C4CC09180A>.
- M.K. Karunananda, N.P. Mankad, Heterobimetallic H₂ addition and alkene/alkane elimination reactions related to the mechanism of E-selective alkyne semihydrogenation, *Organometallics* 36 (2017) 220, <https://doi.org/10.1021/acs.organomet.6b00356>.
- U. Jayarathne, T.J. Mazzacano, S. Bagherzadeh, N.P. Mankad, Heterobimetallic complexes with polar, unsupported Cu–Fe and Zn–Fe bonds stabilized by N-heterocyclic carbenes, *Organometallics* 32 (2013) 3986, <https://doi.org/10.1021/om400471u>.
- S. Banerjee, M.K. Karunananda, S. Bagherzadeh, U. Jayarathne, S.R. Parmelee, G. W. Waldhart, N.P. Mankad, Synthesis and characterization of heterobimetallic complexes with direct Cu–M Bonds (M = Cr, Mn Co, Mo, Ru, W) supported by N-heterocyclic carbene ligands: a toolkit for catalytic reaction discovery, *Inorg. Chem.* 53 (2014) 11307, <https://doi.org/10.1021/ic5019778>.
- F.A. Cotton, L.M. Daniels, C.A. Murillo, H.C. Zhou, The effect of divergent-bite ligands on metal–metal bond distances in some paddlewheel complexes, *Inorganica Chim. Acta.* 300–302 (2000) 319, [https://doi.org/10.1016/S0020-1693\(99\)00537-X](https://doi.org/10.1016/S0020-1693(99)00537-X).
- S.R. Parmelee, N.P. Mankad, A data-intensive re-evaluation of semibridging carbonyl ligands, *Dalt. Trans.* 44 (2015) 17007, <https://doi.org/10.1039/C5DT02813B>.

- [38] M.D. Curtis, K.R. Han, W.M. Butler, Metal-metal multiple bonds. 5. Molecular structure and fluxional behavior of tetraethylammonium μ -cyano-bis(cyclopentadienyldicarbonylmolybdate) (Mo-Mo) and the question of semibridging carbonyls, *Inorg. Chem.* 19 (1980) 2096.
- [39] M.K. Karunananda, F.X. Vázquez, E.E. Alp, W. Bi, S. Chattopadhyay, T. Shibata, N.P. Mankad, Experimental determination of redox cooperativity and electronic structures in catalytically active Cu-Fe and Zn-Fe heterobimetallic complexes, *Dalton Trans.* 43 (2014) 13661, <https://doi.org/10.1039/C4DT01841A>.
- [40] A. Hicken, A.J.P. White, M.R. Crimmin, Preparation and characterisation of heterobimetallic copper-tungsten hydride complexes, *Dalton Trans.* 47 (2018) 10595, <https://doi.org/10.1039/C8DT01569D>.
- [41] G.J. Kubas, Dihydrogen complexes as prototypes for the coordination chemistry of saturated molecules, *PNAS* 104 (2007) 6901, <https://doi.org/10.1073/pnas.0609707104>.
- [42] Azwana R. Sadique, Elizabeth A. Gregory, William W. Brennessel, P.L. Holland, Mechanistic insight into NN cleavage by a low-coordinate iron(II) hydride complex, *J. Am. Chem. Soc.* (2007), <https://doi.org/10.1021/JA069199R>.
- [43] R.H. Morris, Estimating the acidity of transition metal hydride and dihydrogen complexes by adding ligand acidity constants, *J. Am. Chem. Soc.* 136 (2014) 1948, <https://doi.org/10.1021/ja410718r>.
- [44] N.P. Mankad, D.S. Laitar, J.P. Sadighi, Synthesis, structure, and alkyne reactivity of a dimeric (carbene)copper(I) hydride, *Organometallics* 23 (2004) 3369, <https://doi.org/10.1021/om0496380>.
- [45] A.J. Jordan, C.M. Wyss, J. Bacsa, J.P. Sadighi, Synthesis and reactivity of new copper(I) hydride dimers, *Organometallics* 35 (2016) 613, <https://doi.org/10.1021/acs.organomet.6b00025>.
- [46] D.A. Brown, H.J. Lyons, A.R. Manning, A new type of isomerism in some phosphine and phosphite derivatives of the metal carbonyls, *Inorg. Chim. Acta* 4 (1970) 428, [https://doi.org/10.1016/S0020-1693\(00\)93320-6](https://doi.org/10.1016/S0020-1693(00)93320-6).
- [47] H.G. Alt, H.E. Engelhardt, W. Kläui, A. Müller, Trimethylphosphan- und Carbonyl-hydrid-Halbsandwichkomplexe des Chroms, Molybdäns und Wolframs: C5Hf5-, C5Me5- und ein isoelektronischer 6e--Sauerstoff-Tripodligand im Vergleich, *J. Organomet. Chem.* 331 (1987) 317, [https://doi.org/10.1016/0022-328X\(87\)80004-9](https://doi.org/10.1016/0022-328X(87)80004-9).
- [48] P. Müller, Practical suggestions for better crystal structures, *Crystallogr. Rev.* 15 (2009) 57, <https://doi.org/10.1080/08893110802547240>.